# Transthoracic Echocardiographic Diagnosis of a Case of Aortopulmonary Window Combined With Pulmonary Artery Sling

Ann. Ital. Chir., 2025 96, 10: 1282–1285 https://doi.org/10.62713/aic.4290

Zhaonian Huang<sup>1</sup>, Chao Tian<sup>1</sup>, HongKui Yu<sup>1</sup>

Accounting for less than 0.1% of all congenital heart disease (CHD), aortopulmonary window (APW) is characterized by an abnormal communication between the ascending aorta (AAo) and the main pulmonary artery (MPA) [1]. With an incidence rate of approximately 0.25%, pulmonary artery sling (PAS) is characterized by an anomalous origin of the left pulmonary artery (LPA) from the right pulmonary artery (RPA) [2], with the LPA coursing posteriorly to the trachea, forming a vascular "sling" that often causes significant airway compression [3]. The coexistence of APW and PAS is even rarer. This report highlights echocardiographic features of concurrent APW-PAS, a rare and complex malformation that requires preoperative airway assessment.

A male infant was delivered at 33+1 weeks' gestation, with a birth weight of 1790 g. The Apgar scores were 9, 10, and 10 at 1, 5, and 10 minutes, respectively. Prenatal imaging suggested PAS. Post-delivery respiratory distress manifested as tachypnea, cyanosis, and apnea, necessitating noninvasive positive pressure ventilation (NIPPV) support. On examination, blood pressure was 60/30 mmHg, heart rate 123 bpm, and respiratory rate 65/minute. He exhibited no cyanosis or clubbing and an unremarkable cardiopulmonary exam.

Multiplanar transthoracic echocardiography (TTE) findings of the patient are as follows: Bedside scans used a Mindray M9 system with P10-4s and C10-3s probes, whereas comprehensive exams used a Philips EPIQ CVx with S9-2 (pediatric sector) and eL18-4 (linear) probes. Presets followed the American Society of Echocardiography standards. Color Doppler was optimized with a Nyquist limit of 30 cm/s and a wall filter of 50–100 Hz. Initial echo revealed flow signals consistent with secundum atrial septal defects (ASD) and perimembranous ventricular septal defects (VSD). Parasternal short-axis view showed echo dropout in the distal aortopulmonary septum measuring 7.2 mm in diameter; the defect-to-MPA ratio was 1.0, with "T-shaped" artifact margins (Fig. 1A). High left paraster-

Submitted: 8 August 2025 Revised: 27 August 2025 Accepted: 2 September 2025 Published: 10 October 2025

Correspondence to: Zhaonian Huang, Department of Ultrasound Medicine, Shenzhen Baoan Women's and Children's Hospital, 518101 Shenzhen, Guangdong, China (e-mail: znhuang666@163.com).

nal long-axis and subcostal views confirmed a true defect rather than parallel-beam dropout. Color Doppler demonstrated a low-velocity shunt (Fig. 1B). Pulmonary hypertension (PH) was evident, indicated by a peak tricuspid regurgitation (TR) velocity of 4.09 m/s, corresponding to a gradient of 66 mmHg, alongside holodiastolic flow reversal in the descending aorta. Tricuspid annular plane systolic excursion (TAPSE) measured 6 mm and right ventricular fractional area change (RVFAC) was 39%. Lung ultrasound revealed pulmonary edema changes, suggesting pulmonary hyperperfusion. Systemic hypoperfusion was suspected based on hemodynamic assessment. Imaging confirmed an anomalous origin of the LPA from the distal RPA rather than the MPA, with an internal diameter of 4.7 mm and a Pediatric Heart Network (PHN) Z-score of +0.794.

In view of the findings, we reached a final diagnosis for this case, which included an APW, PAS, VSD, ASD and PH. These anomalies were confirmed by digital subtraction angiography (DSA). And cardiac computed tomography (CT) angiography with three-dimensional (3D) reconstruction corroborated complex CHD, including a PAS with tracheal compression, ASD, VSD, PH and a window-type PDA (which was later intraoperatively confirmed as an APW).

On postnatal day 65, at a corrected gestational age (CGA) of 41+5 weeks (i.e.,41 weeks and 5 days), the first surgical procedure was conducted, involving APW closure using a patch technique, ectopic LPA dissection and end-to-side anastomosis to the MPA, and repair of the VSD. Postoperatively, the patient experienced persistent hemodynamic instability, frequent episodes of hypoxia, and an inability to extubate, which necessitated continued invasive mechanical ventilation. On postnatal day 80 (CGA 44+4 weeks), the second surgical procedure was performed, in which emergency definitive surgery was conducted to address tracheal stenosis via resection of the narrowed segment and slide tracheoplasty. Intraoperative findings confirmed preoperative echocardiographic assessments (Fig. 2).

The postoperative course of the patient was favorable, with steady recovery observed. During the first follow-up at approximately one month post-surgery (CGA 2.55 months), weight and length were 4.03 kg and 53.6 cmboth at approximately the 3rd percentile according to the World Health

<sup>&</sup>lt;sup>1</sup>Department of Ultrasound Medicine, Shenzhen Baoan Women's and Children's Hospital, 518101 Shenzhen, Guangdong, China

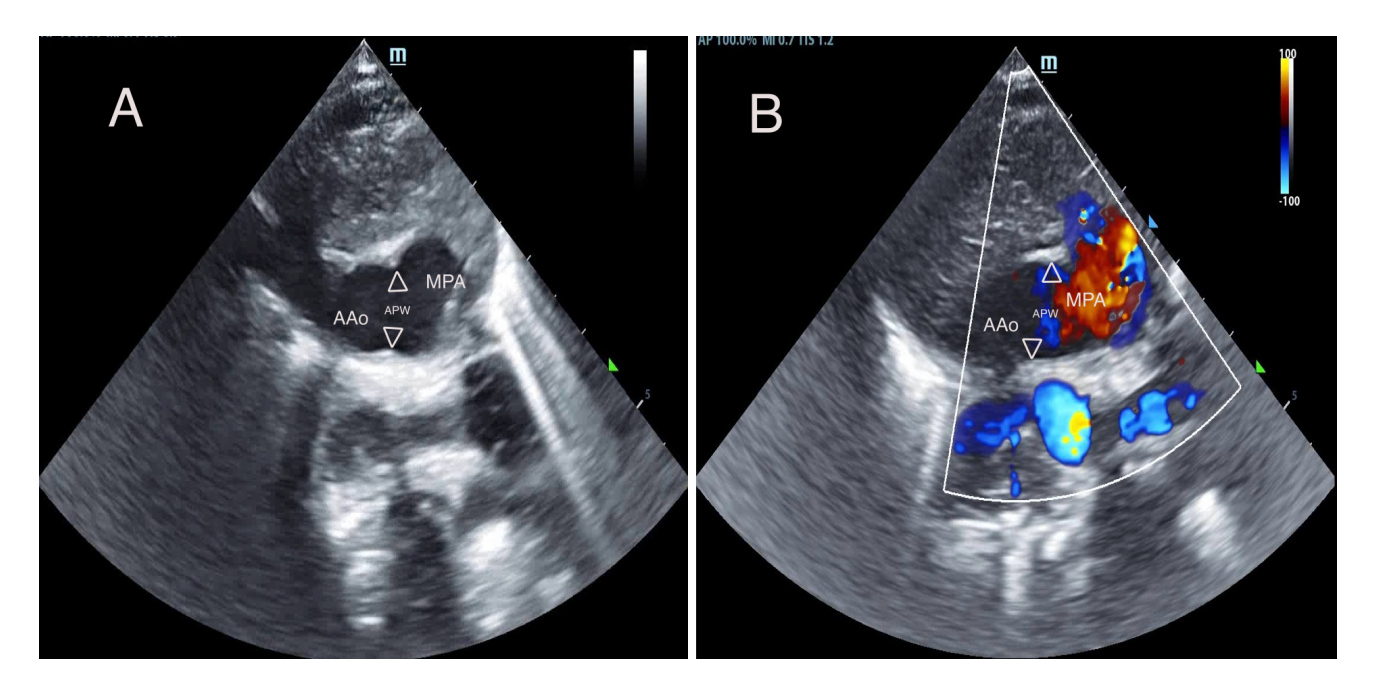


Fig. 1. High parasternal short-axis TTE demonstrating an aortopulmonary window. (A) High parasternal short-axis view of the great arteries shows the defect between the ascending aorta and the pulmonary artery (region between the two white triangles). (B) High parasternal short-axis view of the great arteries shows low-velocity shunt flow between the ascending aorta and the pulmonary artery (region between the two white triangles). Abbreviations: AAo, ascending aorta; APW, aortopulmonary window; MPA, main pulmonary artery.

Organization (WHO) Child Growth standards (2006). At approximately 7 months post-surgery (CGA 9.37 months), the infant recorded a weight of 8.75 kg (41st percentile) and a length of 67.3 cm (3rd percentile). Since no other factors affecting linear growth were identified, we suspected that a prolonged hospitalization (102 days) was the plausible reason for the late catch-up in growth for this patient. Follow-up TTE demonstrated no residual shunting at the great arteries and a normal LPA internal diameter. Pre-discharge bronchoscopy after the second operation confirmed patency of the main, right, and left bronchi. Within 7 months post-surgery, the infant patient exhibited no persistent wheeze or recurrent infections. Mid-term follow-up with CTA/bronchoscopy (6–12 months) was planned to assess airway remodeling.

This case is particularly noteworthy due to the coexistence of two rare congenital cardiac anomalies—APW and PAS—which considerably complicated both diagnosis and management. Based on the Mori classification, the APW was identified as Type II (distal type), while it also showed features consistent with Type B in the Berry classification [4]. The defect's proximity to the origin of the RPA further contributed to the diagnostic difficulty during echocardiographic evaluation. It can mimic a large patent ductus arteriosus (PDA) in high left parasternal "ductal arch" views when the defect's size approximates the MPA diameter.

Owing to its rapid, non-invasive, and bedside applicability, TTE is a valuable tool for the assessment of congenital heart disease. However, this approach has limitations in cases of

pulmonary hypertension coupled with elevated vascular resistance, as reduced shunt flow velocities can diminish the sensitivity of color Doppler imaging. This often results in weak/absent shunt signals, which can be misinterpreted as artifacts or missed entirely. In this case, APW was repeatedly mistaken for artifacts or PDA—misinterpretations that cause surgical delay. Therefore, we recommend prompt use of supplementary imaging modalities—such as CT angiography, DSA, or transesophageal echocardiography—in cases of uncertain echocardiographic drop-out, particularly when accompanied by severe respiratory symptoms. According to statistics, CT angiography achieves a 100% sensitivity, outperforming TTE (78.6%) in a surgical-reference cohort; conversely, for intracardiac defects, TTE is superior (92.5% vs. 84.5%) [5]. Optimal ultrasound technique requires meticulous multiplanar scanning and Doppler parameter adjustments. Although the parasternal short-axis view is often the primary echocardiographic window for detecting APW, supplementary views (such as the high left parasternal/subxiphoid) are required to differentiate true anatomical defects from imaging artifacts. If color Doppler assessment is inconclusive, indirect indicators such as signs for PH and diastolic flow reversal in the descending aorta should be assessed. It has been shown that the absence of pulmonary bifurcation on aortic short-axis view suggests PAS, and TTE using quantitative the distance from the bifurcation of both pulmonary arteries to the pulmonary valve annulus (DBP) or DBP/BSA thresholds (cutoffs: 1.87 cm or 7.68 cm/m<sup>2</sup>, respectively) has a sensitivity of 98–99% and a

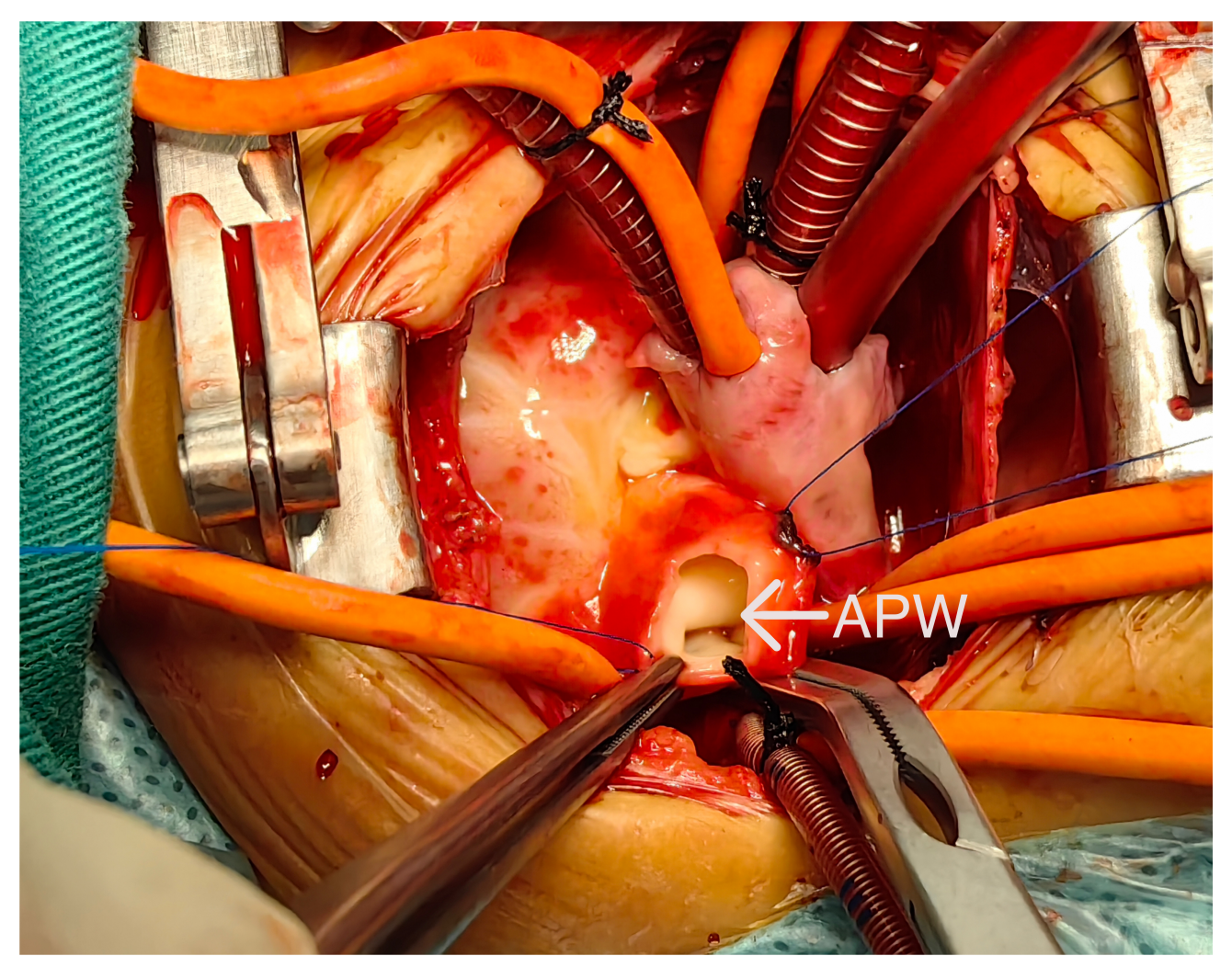


Fig. 2. Intraoperative image showing the aortopulmonary septal defect exposed after opening the anterior wall of the aorta. The white arrow indicates the area of absent septation between the aorta and the pulmonary artery. APW, aortopulmonary window.

specificity of 84–92% [6]. Differentiation of the LPA from a prominent ductus arteriosus can be achieved by assessing flow direction.

The PAS is often accompanied by severe airway abnormalities, including severe tracheal stenosis, complete tracheal rings, and tracheobronchomalacia. Airway disease strongly influences outcomes in PAS. In the present case, bronchoscopy demonstrated a ~30 mm stenotic segment with a minimal inner diameter of ~2 mm, meeting commonly cited thresholds for slide tracheoplasty (e.g., minimum diameter <3 mm and/or stenotic-length/total-length ratio >60%; diameter/length ratio <5.9). A dual-pillar strategycombining low-dose axial imaging (computed tomography angiography (CTA)/4D-CT) for objective anatomical assessment plus staged dynamic bronchoscopy as the reference standard—facilitates accurate delineation of disease extent and determination of optimal timing for combined cardiac-airway repair [7,8].

It is important to note that lower body weight is associated with higher operative risk [9,10]; therefore, surgical inter-

ventions were deferred until the infant achieved a weight of approximately 2.7 kg, with stable hemodynamics and controlled infection. In cases of combined APW and PAS, early single-stage repair-including APW closure, LPA reimplantation and slide tracheoplasty—is advisable when a large left-to-right shunt is present with pulmonary hypertension, hypoxemia or significant airway compromise. If airway symptoms are mild and circulation is controllable, short-term optimization toward a corrected gestational age of approximately 39 weeks and a weight of >2.5-3.0 kg may balance the risks associated with delaying APW repair against the challenges of operating at very low body weight.

Imaging revealed a discrepancy between APW and PDA, although the margins were indistinct. Following a multidisciplinary team review involving cardiac surgery, radiology, and catheterization teams, additional catheter angiography was conducted, providing definitive anatomical evidence pointing to type II (distal) APW, which prompted an adjustment to the surgical plan. Postoperative instability/hypoxia in this case was likely attributable to inadequate preoperative multidisciplinary team evaluation and management of dynamic airway disease, leading to residual symptoms and the need for reintervention. During reoperation, intraoperative bronchoscopy facilitated precise identification of the stenotic segment, and immediate postoperative assessment confirmed an excellent anastomosis. These events underscore the importance of comprehensive multidisciplinary assessment and collaborations between cardiothoracic surgeons, pulmonologists and anesthesiologists.

In summary, the results of this case study demonstrated that the TTE offers a rapid, non-invasive, and effective means for diagnosing the rare coexistence of APW and PAS, even during the neonatal period. Multiplanar scanning and hemodynamic assessment are key to accurate diagnosis. Comprehensive preoperative airway evaluation is pivotal for determining the appropriateness of single-stage versus staged repair and improving patient outcomes.

### Availability of Data and Materials

All data generated or analyzed during this short report are included in this published article. De-identified images are available from the corresponding author on reasonable request.

## **Author Contributions**

Conception and design, ZNH and HKY; collected the clinical data and writing—original draft preparation, ZNH and CT; participated in the clinical diagnosis and treatment of the patient, ZNH, CT, and HKY; writing—review and editing, HKY. All authors contributed to the critical revision of the manuscript for important intellectual content. All authors read and approved the final manuscript. All authors have participated sufficiently in the work and agreed to be accountable for all aspects of the work.

#### **Ethics Approval and Consent to Participate**

The patient's legal guardians provided her informed consent to publication of this report. This report was performed according to the Declaration of Helsinki. This study was approved by the Medical Ethics Committee of Shenzhen Baoan Women's and Children's Hospital (No. LLSC-2025-03-09-07-KS).

#### Acknowledgment

We thank the pediatric cardiology and radiology teams at Shenzhen Baoan Women's and Children's Hospital for their assistance.

## **Funding**

This research received no external funding.

# **Conflict of Interest**

The authors declare no conflict of interest.

#### References

- Alsoufi B, Schlosser B, McCracken C, Kogon B, Kanter K, Border W, et al. Current Outcomes of Surgical Management of Aortopulmonary Window and Associated Cardiac Lesions. The Annals of Thoracic Surgery. 2016; 102: 608–614. https://doi.org/10.1016/j.athoracsur.2016.02.035.
- [2] K Rahmath MR, Durward A. Pulmonary artery sling: An overview. Pediatric Pulmonology. 2023; 58: 1299–1309. https://doi.org/10. 1002/ppul.26345.
- [3] Berdon WE, Baker DH, Wung JT, Chrispin A, Kozlowski K, de Silva M, et al. Complete cartilage-ring tracheal stenosis associated with anomalous left pulmonary artery: the ring-sling complex. Radiology. 1984; 152: 57–64. https://doi.org/10.1148/radiology.152.1. 6729137.
- [4] Gužvinec P, Muscogiuri G, Hrabak-Paar M. CT Assessment of Aortopulmonary Septal Defect: How to Approach It? Journal of Clinical Medicine. 2024; 13: 3513. https://doi.org/10.3390/jcm13123513.
- [5] Xiao HJ, Zhan AL, Huang QW, Huang RG, Lin WH. Accuracy and image quality of wide-detector revolution CT angiography combined with prospective ECG-triggered CT angiography in the diagnosis of congenital aortic arch anomalies in Chinese children. Frontiers in Pediatrics. 2022; 10: 1017428. https://doi.org/10.3389/fped.2022. 1017428.
- [6] Xu QC, Liu JF, Xie M, Weng ZJ, Chen Q, Guo S. Prediction of pulmonary artery sling in children using echocardiography: scoring based on pulmonary artery bifurcation and pulmonary valve ring distance. Cardiovascular Ultrasound. 2025; 23: 5. https://doi.org/10. 1186/s12947-025-00340-8.
- [7] Yong MS, Zhu MZL, Bell D, Alphonso N, Brink J, d'Udekem Y, et al. Long-term outcomes of surgery for pulmonary artery sling in children. European Journal of Cardio-thoracic Surgery. 2019; 56: 369–376. https://doi.org/10.1093/ejcts/ezz012.
- [8] Harada A, Shimojima N, Shimotakahara A, Azuma S, Ishizuka Y, Tomita H, et al. Surgical indication for congenital tracheal stenosis complicated by pulmonary artery sling. Journal of Thoracic Disease. 2019; 11: 5474–5479. https://doi.org/10.21037/jtd.2019.11.31.
- [9] Kalfa D, Krishnamurthy G, Duchon J, Najjar M, Levasseur S, Chai P, et al. Outcomes of cardiac surgery in patients weighing <2.5 kg: affect of patient-dependent and -independent variables. The Journal of Thoracic and Cardiovascular Surgery. 2014; 148: 2499–2506.e1. https://doi.org/10.1016/j.jtcvs.2014.07.031.</p>
- [10] Anderson BR, Blancha Eckels VL, Crook S, Duchon JM, Kalfa D, Bacha EA, et al. The Risks of Being Tiny: The Added Risk of Low Weight for Neonates Undergoing Congenital Heart Surgery. Pediatric Cardiology. 2020; 41: 1623–1631. https://doi.org/10.1007/s00246-020-02420-0.

© 2025 The Author(s).

